trosymmetric pairs and designated I(21), I(22), and I(23), are also near the hexamer with the closest approaches being to the N(3) pyrimidinium positions at 3.59–3.73 Å. Both of the disordered positions for Hg(2) are within bonding distance of I(21), I(22), and I(23), while only one of them, Hg(2a), is bound to I(24). Upon comparison of the Hg–I bond distances (Table I) and angles (Table II) with those previously reported for $[HgI_4]^{2-}$[7,8] and $[HgI_3]^-$,[8,9] we concluded that two anions, $[HgI_4]^{2-}$ and $[(DMSO)HgI_3]^-$, are associated with the hexamer, one to the right and one to the left, as shown in Figure 2. However, since I(24) occupies a center of symmetry, these two anions are disordered in the lattice with each taking the left-hand position in half of the unit cells and the right-hand position in the remaining half. The Hg(II) ion in the $[HgI_3]^-$ ion is further coordinated by DMSO 6 at a Hg(2b)–O(6) distance of 2.75 (5) Å, which is longer than Hg–O separations in similar compounds.[10]

A third anion, $[Hg_2I_7]^{3-}$, is located in the lattice, fairly isolated from any other component of the structure (Figure 2). This is to our knowledge the first structural report of this mercury(II) polyiodide ion. The geometry about the Hg(1) ion is nearly tetrahedral (Table I), and the bridging I(14) is located on an inversion center. The bridging role of I(14) results in a Hg(1)–I(14) distance about 0.15 Å longer than the average terminal Hg(1)–I distance. This is consistent with what is observed in $[Hg_2I_6]^{2-}$.[11] Accordingly, the terminal I–Hg(1)–I(14) [I = I(11), I(12), I(13)] angles are significantly smaller than the remaining I–Hg(1)–I angles (Table II).

In addition to the DMSO that is coordinated to Hg(2b), there are 11 other DMSO molecules in the lattice. One of these is inversion-related to the DMSO that coordinates Hg(2b) and is loosely held, which probably accounts for the disorder found for DMSO 6. Six of the DMSO molecules, numbers 2, 4, and 5, form a "belt" around the exterior of the hexamer, with each DMSO oxygen forming a hydrogen bond to N(41) of one ring, with O–N distances ranging from 2.66 to 2.80 Å while also approaching N(1) of an adjacent pyrimidinium ring with O–N distances of 2.79–3.11 Å. Four more DMSO molecules, numbers 1 and 3, are located above and below the hexamer and are hydrogen bonded to N(41) groups of only one pyrimidinium ring at 2.83 and 2.82 Å, respectively. The two water molecules hydrogen bond at 3.09 Å to DMSO 2, which is the DMSO that hydrogen bonds most weakly to the hexamer.

The general features of the ^1H NMR spectrum reported here are similar to those observed for (24-pyrimidinium crown-6)$(NO_3)_6$,[12] except for the signals due to the C(35) protons, for which we report here an AB quartet rather than the singlet observed for (24-pyrimidinium crown-6)$(NO_3)_6$. The two protons of the C(35) methylene group are not equivalent in the static structure of the hexamer. However, rapid torsion about the C(5)–C(35) and C(35)–N(1) bonds creates an average mirror plane perpendicular to the pseudo-3-fold axis of the hexamer. Such rapid rotation apparently occurs in the nitrate salt of the hexamer but not in the compound reported here. We believe this indicates that the polyiodomercurate anions remain associated with the hexamer in solution, thus blocking the ring flexing motion and producing the observed AB quartet.

With its high positive charge and large central cavity, (24-pyrimidinium crown-6)$^{6+}$ is an attractive candidate for anion complexation. Other notable properties are the ease of synthesis, minimal flexibility due to the aromatic rings, and the presence of both H-bond acceptor, N(3), and donor, N(41), sites. This work demonstrates that an iodide anion can fit into the cavity and that species such as $[HgI_4]^{2-}$ and $[(DMSO)HgI_3]^-$ will associate with this hexameric cation. In addition, a new anion, $[Hg_2I_7]^{3-}$, is seen here in the lattice, presumably as a result of the high positive charge on (24-pyrimidinium crown-6). Work with a number of other anions is in progress.

Supplementary Material Available: Listings of positional and thermal parameters, least-squares planes, bond distances and angles, and hydrogen bonds (10 pages); a table of final observed and calculated structure factors (8 pages). Ordering information is given on any current masthead page.

(7) McAuliffe, C. A. *The Chemistry of Mercury*; McAuliffe, C. A., Ed.; MacMillan: London, 1977.
(8) Deacon, G. B. *Rev. Pure Appl. Chem.* **1963**, *13*, 189.
(9) Fenn, R. H.; Oldham, J. W. H.; Phillips, D. C. *Nature* **1963**, *198*, 381.
(10) In $[\mu$-(DMSO)$HgCl_2]_2$, the Hg–O distances are 2.52 and 2.56 Å: Biscarini, P.; Fusina, L.; Nivellini, G. D.; Mangia, A.; Pelizzi, G. *J. Chem. Soc., Dalton Trans.* **1974**, 1846.
(11) In $(I)_2Hg(I)_2Hg(I)_2$, the two terminal Hg–I distances average 2.69 Å, while the bridging Hg–I bonds range from 2.880 (4) to 2.950 (4) Å: Beurskens, P. T.; Bosman, W. P. J. H.; Cras, J. A. *J. Cryst. Mol. Struct.* **1972**, *2*, 183.
(12) Kim, E., M.S. Thesis, University of Hawaii, 1987.

Contribution from the Department of Chemistry, University of Florida, Gainesville, Florida 32611

Oxidation of Alcohols by a Six-Coordinate Ru(IV)–O Complex

Thomas R. Cundari† and Russell S. Drago*

Received October 25, 1989

Introduction

Much research has been conducted on the mechanisms by which metal–oxo reagents oxidize organic substrates.[1] Many of the proposed mechanisms involve attack of the substrate on the oxo and oxidation of the substrate (and reduction of the metal) followed by solvolysis of the oxidized product. For example, INDO/1 analyses of epoxidations[2a] and sulfoxidations,[2b] by the same six-coordinate Ru(IV)–O complex discussed herein, reveal that the favored pathways are directed at the oxo; the metal played no direct role in the oxidation and acted only as an electron sink. The complex *cis*-$[Ru(bpy)_2(py)(O)]^{2+}$ is active for methanol oxidation.[3] MeOH (and other aliphatic alcohols) oxidation differs in some respects from those of the aromatic alcohols in that its $\Delta H^{\ddagger}$ (14 ± 2 kcal mol^{-1}) is higher than that of benzyl alcohol (5.7 ± 0.2 kcal mol^{-1}).[3] Unlike that of benzyl alcohol, the enthalpy of activation for methanol is temperature dependent, although only a small temperature range was studied (291–313 K). For MeOH, k_H/k_D = 9; the k_H/k_D for benzyl alcohol is 50![3] The rates of oxidation of benzylic alcohols are about 2 orders of magnitude greater than those for aliphatic alcohols.[3] As Meyer has proposed, the extremely high kinetic isotope effect may result from quantum-mechanical tunneling, but only in significant amounts for the benzylic alcohols while the aliphatic alcohols proceed through a classical pathway. This present study extends the previous research to the oxidation of alcohols by a Ru(IV)–O complex.[4] The intent is to see if a substrate which is a good donor will prefer pathways that directly involve the metal in the oxidation. Similar proposals have been discussed with respect to the mechanism of olefin epoxidation by η^2-peroxides.[5a,b] The mechanism for this reaction has been envisaged to occur by either precoordination of the olefin to the metal followed by addition of the metal–oxygen bond across the double bond of the olefin to yield a five-membered-ring intermediate[5a] or direct attack of the olefin on a peroxide oxygen followed by electronic rearrangement to yield epoxide product.[5b] The preferred pathway as revealed by an extended Hückel analysis of epoxidation by η^2-peroxides involves precoordination of the substrate to the metal followed by attack on a peroxide oxygen; i.e. it is a combination of both proposals.[5c]

Calculations

An MO analysis of the interaction between *cis*-$[Ru(HN{=}CH{-}HC{=}NH)_2(NH_3)(O)]^{2+}$ (hereafter referred to as RuN_5O^{2+}, Figure 1) and methanol was performed by using the INDO/1 method.[6] The calculation of open- and closed-shell species employed the unrestricted

† Present address: Department of Chemistry, North Dakota State University, Fargo, ND 58105-5516.

0020-1669/90/1329-3904$02.50/0

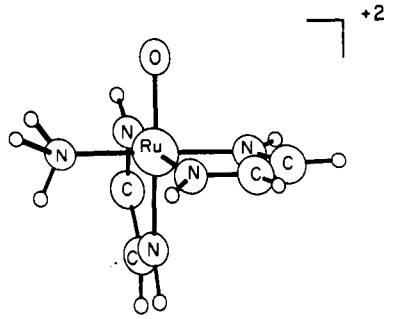

Figure 1. $[Ru(NH{=}CH{-}CH{=}NH)_2(NH_3)(O)]^{2+}$ complex used in the calculations to model the experimentally employed complexes.

Table I

1. Methanol Geometry[7]
R(CH) = 1.096 Å, R(CO) = 1.427 Å, R(OH) = 0.956 Å
θ(HCH) = 109.03°, θ(HOC) = 108.9°

2. $Ru(NH{=}CH{-}CH{=}NH)_2(NH_3)(O)^{2+}$ Geometry

a. Glyoxal Diimine[7]
R(NH) = 1.01 Å, R(CH) = 1.09 Å, R(NC) = 1.35 Å, R(CC) = 1.50 Å
θ(NCC) = 116.1°

b. Ammonia[7]
R(NH) = 1.012 Å
θ(HNH) = 106.67°

c. Other[a]
R(RuN) = 2.06 Å, R(RuO) = 1.96 Å

[a] Obtained from a geometry optimization of RuN_5O^{2+}.

Hartree–Fock formalism[7] to allow for the direct comparison of properties. The pertinent bond lengths and bond angles for RuN_5O^{2+} were obtained from bipyridine[8] and free ammonia[8] for the glyoxal diimine, HN=C-H—HC=NH, and ammonia ligands, respectively. Further geometric details are given in Table I.

Results and Discussion

The electronic structure of the RuN_5O^{2+} complex has been discussed previously from theoretical[3] and experimental[9] points of view. The key features involve a half-filled, nearly degenerate pair of covalent Ru dπ–O pπ antibonding frontier orbitals underscoring a similarity with O_2 in terms of low-energy triplet and singlet states.[9] The formal oxidation state on the Ru is +4, yielding a d^4 metal.

1. Interaction between the Reactant Fragments. a. C–H Activation at the Oxo Moiety. Two limiting trajectories for the interaction of the C–H bond of MeOH with oxo were considered—a linear C–H/Ru-oxo pathway, **1a**, and a perpendicular path, **1b** (Scheme I). The term oxo will be used to refer to the terminal oxygen coordinated to ruthenium. A potential curve for each C–H activation pathway was constructed as follows. First, the reactant geometries were kept fixed. Single-point INDO/1 calculations were used to evaluate properties at various fragment separations from R_{oxo-H} = 3.20 Å to R_{oxo-H} = 0.94 Å in approximately 0.10-Å increments. The perpendicular trajectory, **1b**, was calculated to be repulsive at all separations and is discussed no further.

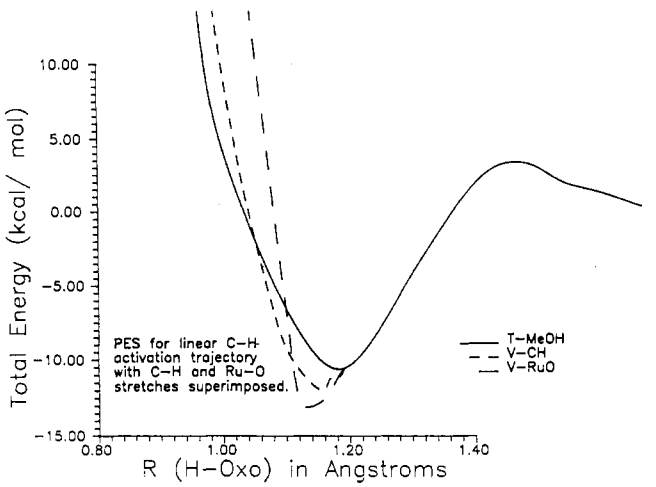

Figure 2. Potential energy curve for the translation of the entire methanol fragment relative to the Ru–oxo fragment in a linear orientation and with C–H and Ru–O stretching vibrations imposed upon the ion–molecule minimum.

Scheme I. Linear (**1a**) and Perpendicular (**1b**) Addition Modes of a Methanol C–H Bond to the Oxo Portion of the Ru–Oxo Moiety at Different Interaction Strengths

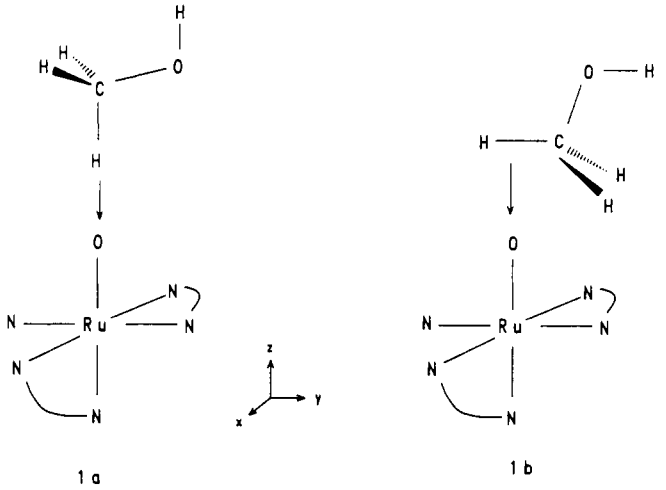

The energy for RuN_5O^{2+}·MeOH (linear pathway) is equal to the sum of the energies of isolated reactants (Figure 2) when $R_{oxo-H} \geq 1.7$ Å. At $R_{oxo-H} \approx 1.4$ Å, the sum of the ionic radii of O^{2-} and H^+,[10] a barrier of 3.1 kcal mol^{-1} to further translation of the methanol (Figure 2) is found originating from a repulsive interaction between the oxo lone pair (predominantly O $2p_z$) and the methanol C–H σ bond. At R_{oxo-H} = 1.20 Å (Figure 2), there is a minimum which is calculated to be 10.6 kcal mol^{-1} below reactants. Shortening of R_{oxo-H} beyond 1.20 Å causes a large increase in the total energy. The linear complex resembles a hydrogen bond. The RuN_5O^{2+}·MeOH interaction is significant, but these are calculations on gas-phase systems and in solution this species has to compete with the interaction of the solvent molecules around the complex (water or alcohol). Formation of

(1) Holm, R. H. *Chem. Rev.* **1987**, *87*, 1401 and references therein.
(2) (a) Cundari, T. R.; Drago, R. S. *Inorg. Chem.* **1990**, *29*, 487. (b) The INDO/1 results for organic sulfide oxidations by the model RuN_5O^{2+} (Cundari, T. R. Ph.D. Dissertation, University of Florida, May 1990) are what one would expect. The experimental results are outlined in: Roecker, L.; Dobson, J. C.; Vining, W. J.; Meyer, T. J. *Inorg. Chem.* **1987**, *26*, 779.
(3) (a) Roecker, L.; Meyer, T. J. *J. Am. Chem. Soc.* **1987**, *109*, 746. (b) Thompson, M. S.; Meyer, T. J. *J. Am. Chem. Soc.* **1982**, *104*, 4106.
(4) Cundari, T. R.; Drago, R. S. *Int. J. Quantum Chem.* **1989**, *23*, 489 (Proceedings of the 1989 Sanibel Symposium).
(5) (a) Mimoun, H.; Seree de Roch, I.; Sajus, L. *Tetrahedron* **1970**, *26*, 37. (b) Sharpless, K. B.; Townsend, J. M.; Williams, D. R. *J. Am. Chem. Soc.* **1972**, *94*, 295. (c) Hoffmann, R.; Jorgensen, K. A. *Acta Chem. Scand.* **1986**, *B40*, 411.
(6) (a) Bacon, A. D.; Zerner, M. C. *Theor. Chim. Acta* **1979**, *52*, 21. (b) Anderson, W. P.; Edwards, W. D.; Zerner, M. C. *Inorg. Chem.* **1986**, *25*, 2728. (c) Pople, J. A.; Beveridge, D. L. *Approximate Molecular Orbital Theory*; McGraw-Hill: New York, 1970. (d) Cundari, T. R.; Zerner, M. C.; Anderson, W. P.; Drago, R. S. *Inorg. Chem.* **1990**, *29*, 1.
(7) Pople, J. A.; Nesbet, R. K. *J. Chem. Phys.* **1954**, *22*, 571.
(8) Sutton, L. E. *Interatomic Distances*; Chemical Society: London, 1958; p S8.
(9) Dobson, J. C.; Helms, J. H.; Doppelt, P.; Sullivan, B. P.; Hatfield, W. E.; Meyer, T. J. *Inorg. Chem.* **1989**, *28*, 2200.
(10) (a) Chambers, C.; Holliday, A. K. *Modern Inorganic Chemistry*; Butterworths: London, 1979; p 258. (b) The assumption of zero radius for the proton goes back at least as far as Lewis. See, e.g.: Lewis, G. N. *Valence*; Chemical Catalog Co.: New York, 1923; p 120.

a weakly bound species would be difficult in solution.

Three geometric perturbations from the minimum were explored to study hydrogen transfer, i.e. C–H stretching (at constant R_{Ru-oxo}), Ru–O stretching (at R_{C-H}), and simultaneous stretching of Ru–O and C–H. The first two perturbations cause large increases in the total energy.[11a] For the last perturbation the C–H and Ru–oxo bonds were stretched by 0.12 Å each,[11b] starting with the ion–molecule complex, leading to an increase in the total energy by 52 kcal mol^{-1} (≈4 times the experimental[3] $\Delta H^{\ddagger}$).

b. Seven-Coordinate Structures. There is a pattern of two lower and three higher energy frontier orbitals (largely metal d in character) for seven-coordinate complexes.[12] Thus d^4 ML_7 complexes should be relatively stable. The larger size of second-row transition-metal atoms also increases the possibility of a seven-coordinate intermediate or transition state. Experimentally,[3] there is a large, negative $\Delta S^{\ddagger}$ for the oxidation of MeOH by *cis*-$[Ru(bpy)_2(py)(O)]^{2+}$, indicating that a strongly associated complex exists in the rate-determining step. Ru(IV) seven-coordinate complexes have been reported by Pignolet and coworkers.[13] These facts suggest that an alcohol coordination pathway may be a viable alternative, or competing pathway, to the C–H activation scheme.

Three seven-coordinate structures were investigated—the pentagonal bipyramid (PBP7), the capped octahedron, and the capped trigonal prism. For reasons of brevity, only the PBP7 (found to be the most favorable) will be discussed. The PBP7 complex is formed from the octahedral oxidant in two steps. First, the equatorial plane is expanded to accommodate five instead of four ligands. The distortion of the equatorial N–Ru–N angles from those of the octahedral RuN_5O^{2+}, i.e. N_{eq}–M–$N_{eq} \approx 90°$, to those of a PBP7 complex with the fifth equatorial ligand missing, i.e. N_{eq}–M–$N_{eq} \approx 72°$, costs 9.6 kcal mol^{-1}. The bond lengths were kept constant during this angular deformation. The species in which the fifth equatorial coordination site remains vacant is referred to as the PBP7 precursor; its ground state is a triplet. The second step in the formation of the seven-coordinate $RuN_5O(ROH)^{2+}$ complex entails coordination of MeOH to the vacant equatorial site of the PBP7 precursor. The geometries of the oxidant and substrate were kept constant in those calculations that studied the coordination of the alcohol to the PBP7 precursor. The Ru–O(MeOH) distance was varied from 3.00 to 2.00 Å in ≈0.05-Å increments. The calculations indicate no activation barrier for MeOH coordination. The total energy decreases as R_{MO} decreases until a strongly bound seven-coordinate species is formed—R_e(RuO) = 2.35 Å, binding energy = 30.0 kcal mol^{-1}. The stronger binding energy for the metal-bound alcohol complex versus the linear C–H–oxo pathway directed at the metal compared to that found for the linear C–H–oxo species will allow the former complex to more effectively compete with the solvent molecules around the oxidant.

Several arguments can be made against a seven-coordinate structure:[3] no precedent exists for coordination sphere expansion, rate of ^{18}O exchange (between RuN_5O^{2+} and $^{18}OH_2$) is slow, and no spectrophotometric evidence exists for a seven-coordinate intermediate. As mentioned previously, there are precedents that allow one to propose a seven-coordinate association complex. First, simple frontier MO considerations point to stability for d^4 seven-coordinate complexes.[12] Second, ML_7 d^4 complexes of Ru have been characterized.[13] Furthermore, a small concentration of a reactive seven-coordinate species could be kinetically important in oxidation without being detected spectrophotometrically. With regard to ^{18}O exchange, water would be expected to form association complexes, since it is a ligand comparable to alcohols and sterically less demanding. However, H transfer may not occur for some reason to produce a dihydroxy complex, which will lead to a scrambling of the oxygens. Furthermore, if we assume that the scrambling is accomplished by an intramolecular H transfer, then the fact that the two OH groups are in symmetry-inequivalent positions could incur some obstacle that leads to the unobserved scrambling.

Scheme II. Structure of the "Cyclic" Intermediate Which Combines the C–H–Oxo and M–O Pathways

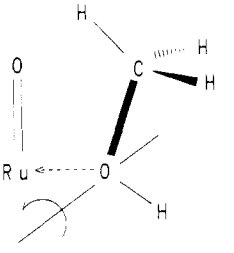

2

2. Further Reaction of the Association Complex. The reported mechanism[3] is given in eqs 1–3. This mechanism entails initial association (eq 1), followed by "hydride" transfer (eq 2, rate

$$N_5Ru{-}O^{2+} + HC(OH)R_2 \rightleftarrows N_5Ru{-}O^{2+},HC(OH)R_2 \quad (1)$$

$$N_5Ru{-}O^{2+},HC(OH)R_2 \rightarrow [N_5Ru{-}O{\cdots}H{-}C(OH)R_2]^{2+} \rightarrow 7N_5Ru{-}OH^{+},C(OH)R_2^{+} \quad (2)$$

$$N_5Ru{-}OH^{+},C(OH)R_2^{+} \rightarrow N_5Ru(OH_2)^{2+} + O{=}CR_2 \quad (3)$$

determining step), and then proton transfer (eq 3). So far, we have dealt with eq 1 of the mechanism, i.e. formation of the association complex between the substrate and the oxidant.

If the calculated minimum from the alcohol-coordination pathway is used and the methanol ligand rotated about an axis perpendicular to the H–O–C plane and passing through the oxygen, **2** (Scheme II), a further 38 kcal mol^{-1} of stabilization is calculated as the methyl C–H bond approaches the oxo; the decrease in the total energy is downhill until **2** is formed. The 38 kcal mol^{-1} decrease in energy is almost certainty too large; however, it does point to further stabilization from increasing C–H···oxo interaction. The equilibrium H···oxo distance in the cyclic complex is the same as that calculated (1.2 Å) for the linear C–H activation pathway. Thus, one is left with a cyclic species, **2**, which combines the attributes of both proposals.

The important point about coordinating the MeOH to the Ru is that it "activates" the substrate. The calculated barrier to H transfer from the cyclic species is calculated (once again by stretching the C–H and Ru–O bonds toward each other by 0.12 Å) to be 16 kcal mol^{-1}, in excellent agreement with the experimental $\Delta H^{\ddagger}$ of 14 ± 2 kcal mol^{-1}. The INDO/1 results suggest that **2** is an intermediate, i.e. the association complex that Meyer has proposed as forming in the first part of the oxidation reaction (eq 1) and not a transition state. However, if hydrogen transfer from a methyl hydrogen to the oxo moiety (to go from $RuN_5(O)(MeOH)^{+2}$ to $RuN_5(OH)(CH_2OH)^{2+}$) is the rate-determining step, the transition state will probably have some metal–alcohol interaction. One other main point must be made about the combined C–H···oxo/M–O interaction pathway. In the linear C–H···oxo pathway, the high-energy C–H σ^* MO leads to a repulsive interaction between the C–H bond and the oxo lone pair. Bringing the C–H bond from the side allows for greater interaction between the C–H bond to be activated and the Ru–O π system.

(11) (a) The initial decrease in the total energy from the linear "minimum" is not surprising, since this is not a true minimum (i.e. all degrees of freedom optimized) but a minimum for the translation of methanol relative to the complex with the reactant geometries "frozen". Preliminary work on the use of INDO/1 in the calculation of stretching frequencies has been carried out. For Ru–O a value of 881 cm^{-1} was found in excellent agreement with the values of 792–820 cm^{-1} found for various Ru(IV) complexes (Che, C.-M.; Lai, T.-F.; Wong, K.-Y. *Inorg. Chem.* **1987**, *26*, 2289) and the calculated value of 801 cm^{-1} (from the data in: Krauss, M.; Stevens, W. J. *J. Chem. Phys.* **1985**, *82*, 5584). The calculated C–H stretches are larger (4200 cm^{-1} (calcd) vs 3000–3500 cm^{-1} (exptl)). (b) A typical covalent O–H bond length is 0.96 Å.[7] The oxo–H distance in the linear minimum is 1.20 Å. It was assumed that Ru–oxo and C–H will each stretch by half of the difference (1.20–0.96 = 0.24 Å).

(12) Hoffmann, R.; Beier, B. F.; Muetterties, E. L.; Rossi, A. R. *Inorg. Chem.* **1977**, *6*, 55.

(13) (a) Given, K. W.; Mattson, B. M.; Pignolet, L. H. *Inorg. Chem.* **1976**, *15*, 3152. (b) Wheeler, S. H.; Mattson, B. M.; Miessler, G. L.; Pignolet, L. H. *Inorg. Chem.* **1978**, *17*, 340.

These M $d\pi$–O $p\pi$ MOs characterize the reactivity of most metal–oxo complexes. Groves[14] has concluded on the basis of stereochemistry that in alkane hydroxylation by the related ferryl porphyrin systems such an approach (i.e. the C–H bond approaches the M–O moiety from the side and is directed at the oxo) is expected. In a linear C–H···oxo pathway the C–H bond to be activated is orthogonal to the RuO π MOs, making direct interaction impossible. Another interesting matter in connection with a seven-coordinate pathway is that once the H^- is transferred, the conditions for eq 3, fragmentation of the association complex, are set in place—i.e. a seven-coordinate structure with a d population greater than 4 is formed. Thus, the association complex breaks up and a fast proton transfer occurs to yield products.

The INDO/1 results suggest that a pathway which involves precoordination of the alcohol to the metal is competitive with, if not more favorable than, a pathway which involves C–H activation by the oxo alone. In fact, the INDO/1 analysis indicates that the preferred pathway is a combination of both proposals; i.e. the precoordination of the substrate to the metal activates the MeOH for further reaction. The calculated barrier decreases from 52 kcal mol^{-1} (linear C–H–oxo) to 16 kcal mol^{-1} (cyclic C–H/Ru–oxo).

Given the interest in metal–oxo mediated oxidations, largely as a result of the heme monooxygenases cytochromes P-450,[15,16] the INDO/1 results should serve to remind one that when dealing with the oxidation of substrates which are potentially good donors (e.g. amines and ethers), pathways which involve direct interaction between the substrate and the metal should be considered. Steric requirements brought about by the coordination environment around the metal as well as the substrate must also be considered when one contemplates a direct metal–substrate route. Coordination of the substrate to the metal for those cases in which it occurs will activate the metal toward further reaction.

Acknowledgment. We thank the NSF and Shell Foundation (in the form of a predoctoral fellowship for T.R.C.) for funding and Prof. Michael C. Zerner (Florida) for information about the ZINDO program (written by himself and his collaborators). The assistance of Greg Harris (Florida) in preparing the manuscript and helpful comments by Prof. Thomas J. Meyer (University of North Carolina—Chapel Hill) are gratefully acknowledged.

(14) Groves, J. T.; Nemo, R. S. *J. Am. Chem. Soc.* **1983**, *105*, 6243.
(15) *Cytochrome P-450: Structure, Mechanism and Biochemistry*; Ortiz de Montellano, P. R., Ed.; Plenum: New York, 1986.
(16) *Cytochrome P-450: Structural and Functional Relationships*; Ruckpaul, K., Ed.; Verlag: Berlin, 1984.

Contribution from the Department of Chemistry, University of Iowa, Iowa City, Iowa 52242

Characterization of Ammonia-Ligated Low-Spin Iron(III) Porphyrin Complexes

Yunghee Oh Kim and Harold M. Goff*

Received March 3, 1989

Substituted imidazoles or pyridines readily coordinate to iron(III) porpyrins to form stable bis(amine)-ligated low-spin iron(III) species.[1-3] Although the analogous bis(aliphatic amine) complexes have been observed at low temperature, these ligands are prone to reduce the iron(III) porphyrin complex to the iron(II) derivative at ambient temperature.[4] Mixed complexes with cyanide and aliphatic amine ligands exhibit no tendency for autoreduction.[4] The ammonia ligand is reportedly inert with respect to reduction of iron(III) to iron(II) porphyrins.[5] It is surprising, however, that an ammonia-ligated iron(III) complex has not been described. The diamagnetic iron(II) octaethylporphyrin complex $(OEP)Fe(NH_3)_2$ has been prepared by the reduction reaction of an iron(III) complex, (OEP)FeCl, and hydrazine in 2-picoline.[6] This report describes the generation of the first low-spin iron(III) porphyrin complex with ammonia ligands.

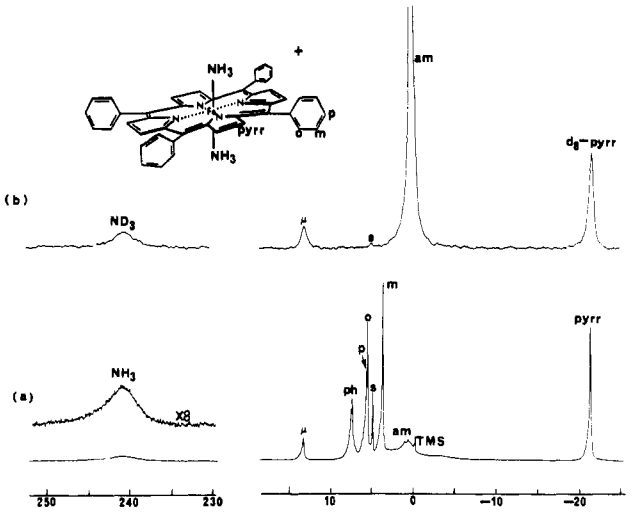

Figure 1. (a) Proton NMR spectrum of a mixture of $(TPP)Fe(NH_3)_2SO_3CF_3$ and $[(TPP)Fe]_2O$ in CD_2Cl_2 solution at 25 °C, referenced to tetramethylsilane in ppm. Signals for $(TPP)Fe(NH_3)_2^+$ are labeled as follows: pyrrole, "pyrr"; ortho, "o"; meta, "m"; para, "p"; coordinated ammonia, "NH_3". Signals for $[(TPP)Fe]_2O$ are labeled "μ" for pyrrole and "ph" for phenyl protons. The solvent signal is labeled "s", free ammonia, "am", and tetramethylsilane, "TMS". (b) Deuterium NMR spectrum of a mixture of $(TPP\text{-}d_8)Fe(ND_3)_2SO_3CF_3$, $[(TPP\text{-}d_8)Fe]_2O$, and excess ND_3 in CH_2Cl_2 solution at 25 °C. Signals are labeled as above.

The ammonia-ligated iron(III) tetraphenylporphyrin (TPP) complex is synthesized by displacement of the weakly coordinated triflate ion in $(TPP)FeSO_3CF_3$ with anhydrous ammonia gas in dichloromethane, chloroform, or toluene solution. Upon introduction of ammonia into a dichloromethane or chloroform solution of $(TPP)FeSO_3CF_3$, the color changes from brown to red (optical bands at 414 (Soret) and 546 nm). When ammonia gas is passed into a toluene solution of $(TPP)FeSO_3CF_3$, the ionic iron porphyrin product precipitates. The solid was recrystallized from dichloromethane and used for NMR and Mossbauer spectroscopic measurements. The iron(III) porphyrin ammonia complex is inevitably contaminated with the thermodynamically stable μ-oxo dimer $[(TPP)Fe]_2O$ due to traces of water in the solvent or ammonia gas.[7] The ammonia complex is stable in the presence of dry oxygen, but the red solution is immediately changed to that of the green μ-oxo dimer when exposed to a moist atmosphere.

Figure 1a shows the proton NMR spectrum of a CD_2Cl_2 solution that contains the ammonia-ligated iron(III) tetraphenylporphyrin complex contaminated with the $[(TPP)Fe]_2O$ byproduct. Phenyl resonances were assigned as follows: ortho, 5.93 ppm; meta, 3.86 ppm; para, 5.77 ppm.[8] The pyrrole proton signal is

(1) Epstein, L. M.; Straub, D. K.; Maricondi, C. *Inorg. Chem.* **1967**, *6*, 1720.
(2) La Mar, G. N.; Walker, F. A. *J. Am. Chem. Soc.* **1972**, *94*, 8607.
(3) Satterlee, J. D.; La Mar, G. N.; Frye, J. S. *J. Am. Chem. Soc.* **1976**, *98*, 7275.
(4) Hwang, Y. C.; Dixon, D. W. *Inorg. Chem.* **1986**, *25*, 3716 and references therein.
(5) Castro, C. E.; Jamin, M.; Yokoyama, W.; Wade, R. *J. Am. Chem. Soc.* **1986**, *108*, 4179.
(6) Dolphin, D.; Sams, J. R.; Tsin, T. B.; Wong, K. L. *J. Am. Chem. Soc.* **1976**, *98*, 6970.
(7) Solvents were rigorously dried and manipulated under a nitrogen atmosphere. Chlorinated solvents were distilled from P_2O_5 under a nitrogen atmosphere. Toluene was distilled from sodium/benzophenone under a nitrogen atmosphere.
(8) These phenyl resonances are assigned from the comparison of the NMR spectra of $(2\text{-}CH_3TPP)Fe(NH_3)_2^+$, $(3\text{-}CH_3TPP)Fe(NH_3)_2^+$, and $(4\text{-}CH_3TPP)Fe(NH_3)_2^+$.

0020-1669/90/1329-3907$02.50/0